Constitutive Activation of the Tumor Suppressor p53 in Hepatocytes Paradoxically Promotes Non–Cell Autonomous Liver Carcinogenesis

Yuki Makino[1], Hayato Hikita[1], Kenji Fukumoto[1], Ji Hyun Sung[1], Yoshihiro Sakano[2], Kazuhiro Murai[1], Sadatsugu Sakane[1], Takahiro Kodama[1], Ryotaro Sakamori[1], Jumpei Kondo[3], Shogo Kobayashi[2], Tomohide Tatsumi[1], and Tetsuo Takehara[1]

ABSTRACT

In chronic liver diseases (CLD), p53 is constitutively activated in hepatocytes due to various etiologies as viral infection, ethanol exposure, or lipid accumulation. This study was aimed to clarify the significance of p53 activation on the pathophysiology of CLDs. In Kras-mutant liver cancer model, murine double minute 2 (Mdm2), a negative regulator of p53, was specifically deleted in hepatocytes [Alb-Cre $Kras^{LSL\text{-}G12D}$ $Mdm2^{fl/fl}$ (LiKM; $Kras^{G12D}$ mutation and Mdm2 loss in the liver)]. Accumulation of p53 and upregulation of its downstream genes were observed in hepatocytes in LiKM mice. LiKM mice showed liver inflammation accompanied by hepatocyte apoptosis, senescence-associated secretory phenotype (SASP), and the emergence of hepatic progenitor cells (HPC). More importantly, Mdm2 deletion promoted non–cell autonomous development of liver tumors. Organoids generated from HPCs harbored tumor-formation ability when subcutaneously inoculated into NOD/Shi-scid/IL2Rγ (null) mice. Treatment with acyclic retinoid suppressed growth of HPCs *in vitro* and inhibited tumorigenesis in LiKM mice. All of the phenotypes in LiKM mice, including accelerated liver tumorigenesis, were negated by further deletion of p53 in hepatocytes (Alb-Cre $Kras^{LSL\text{-}G12D}$ $Mdm2^{fl/fl}$ $p53^{fl/fl}$). Activation of hepatic p53 was noted in liver biopsy samples obtained from 182 patients with CLD, in comparison with 23 normal liver samples without background liver diseases. In patients with CLD, activity of hepatic p53 was positively correlated with the expression of apoptosis, SASP, HPC-associated genes and tumor incidence in the liver after biopsy. In conclusion, activation of hepatocyte p53 creates a microenvironment prone to tumor formation from HPCs. Optimization of p53 activity in hepatocytes is important to prevent patients with CLD from hepatocarcinogenesis.

Significance: This study reveals that activation of p53 in hepatocytes promotes liver carcinogenesis derived from HPCs, which elucidates a paradoxical aspect of a tumor suppressor p53 and novel mechanism of liver carcinogenesis.

See related commentary by Barton and Lozano, p. 2824

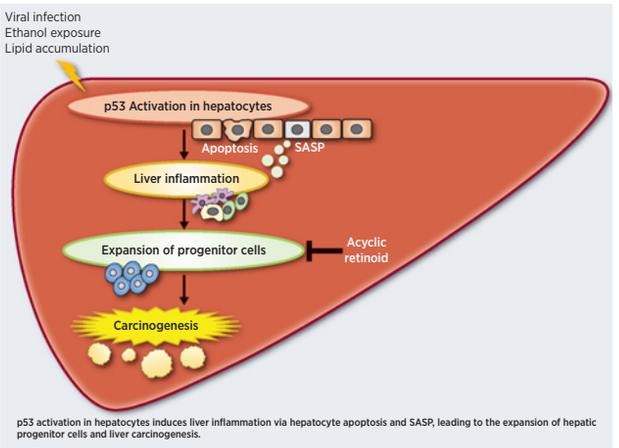

p53 activation in hepatocytes induces liver inflammation via hepatocyte apoptosis and SASP, leading to the expansion of hepatic progenitor cells and liver carcinogenesis.

Introduction

p53, encoded by the TP53 gene, is one of the most important tumor suppressors and is called "a guardian of the genome" (1). The activity of p53 is generally regulated at the protein level through posttranslational modifications (2). Under unstressed conditions, p53 protein levels are usually kept low through continuous degradation (2, 3). The degradation of p53 is mainly mediated by the E3 ubiquitin ligase murine double minute 2 (Mdm2), which ubiquitinates p53 for proteasomal degradation (3). In response to cellular stress, such as DNA damage and oncogene signals, p53 is phosphorylated by several kinases (2, 3). Phosphorylation of p53 inhibits the p53–Mdm2 interaction, resulting in the accumulation of p53 (2, 3). Accumulated p53 acts as a transcription factor and upregulates downstream genes such as p21, bax, and noxa (1–3). Thus, when p53 is activated, it induces cell-cycle arrest, apoptosis, senescence, and DNA repair to prevent carcinogenesis (1–3).

Dysfunction of p53 is involved in a large spectrum of cancer types (1–3). TP53 gene mutation is observed in no less than 50% of

[1]Department of Gastroenterology and Hepatology, Osaka University Graduate School of Medicine, Osaka, Japan. [2]Department of Gastroenterological Surgery, Osaka University Graduate School of Medicine, Osaka, Japan. [3]Department of Molecular Biochemistry and Clinical Investigation, Osaka University Graduate School of Medicine, Osaka, Japan.

Corresponding Author: Tetsuo Takehara, Department of Gastroenterology and Hepatology, Osaka University Graduate School of Medicine, 2-2 Yamadaoka, Suita, Osaka 565-0871, Japan. Phone: 816-6879-3621; Fax: 816-6879-3629; E-mail: takehara@gh.med.osaka-u.ac.jp

Cancer Res 2022;82:2860–73

doi: 10.1158/0008-5472.CAN-21-4390

human cancers. In hepatocellular carcinoma (HCC), the TP53 gene mutation rate is approximately 30%, representing the second most frequent gene mutation in HCC (4, 5). This mutation prevents the p53 protein from binding to the response elements of its target genes. Accumulating evidence suggests that p53 is constitutively activated in hepatocytes in chronic liver disease (CLD) patients with various etiologies (6–15). Every causative agent of CLDs could be involved in p53 activation. The X protein of hepatitis B virus binds to the ubiquitin-binding domain of p53 and prevents p53 degradation (10). The core protein of hepatitis C virus can interact with p53 to enforce its transcriptional activity (11, 12). Ethanol exposure can activate p53 in hepatocytes through reactive oxygen species production (13). Fat accumulation in the liver causes hepatocyte toxicity through excess free fatty acids, oxidative stress, and lipid peroxidation, which could cause activation of hepatocyte p53 (14, 15). Moreover, the influence of p53 activation on the pathophysiology of CLDs has not been sufficiently elucidated thus far.

In the current study, we deleted Mdm2 to constitutively activate hepatocyte p53 in hepatocyte-specific Kras-mutated mice (16). We found that activation of hepatocyte p53 provoked an inflammatory response, accompanied by an increase in hepatocyte apoptosis and a senescence-associated secretory phenotype (SASP). Expansion of hepatic progenitor cells (HPC), a stem-like cell type in the liver (17, 18), was noted in the liver. p53 activation in hepatocytes accelerated the development of liver tumors originating from HPCs, as evidenced by the tumor-formation ability of HPC-derived organoids. In patients with CLD, patients with higher hepatic p53 activity showed increased apoptosis/SASP/HPC-associated gene expression and tumor incidence in the liver. These findings demonstrated that constitutive activation of the tumor suppressor p53 in hepatocytes paradoxically promotes liver carcinogenesis.

Materials and Methods

Human samples

Liver samples were collected by percutaneous biopsy of nontumorous liver tissues. Collected liver tissues were examined for pathologic diagnosis, and surplus samples were used to extract total RNA. Among 266 patients with chronic liver injury who underwent percutaneous liver biopsy from January 2014 to March 2016 and agreed to participate in this study, 84 patients with inadequate specimen amounts for RNA extraction were excluded. The remaining 182 patients with CLD were included, and their clinical background is presented in Supplementary Table S1. Among 51 patients with liver biopsy without underlying liver diseases from June 2014 to August 2019 who agreed to participate in this study, 28 cases without sufficient sample amounts for RNA extraction were excluded. The remaining 23 subjects were included as control normal liver cases, who were patients with metastatic liver tumors ($N = 18$), cholangiocellular carcinoma ($N = 1$), inflammatory pseudotumor ($N = 1$), focal nodular hyperplasia ($N = 1$), a hepatic nodule proven to be normal tissue by biopsy ($N = 1$), and a liver transplantation donor ($N = 1$). Written informed consent was obtained from all subjects. Surgically resected nontumorous liver samples were obtained from patients with HCC or liver metastasis from colorectal cancer and used for IHC as CLD or normal liver samples, respectively. The study protocol followed the ethical guidelines of the Declaration of Helsinki. The use of these samples was approved by the Institutional Review Board (IRB) Committees at Osaka University Hospital (IRB No. 13556 and 15267).

Mice

C57BL/6/129 background mice carrying a transcription termination sequence (loxP-stop-loxP; LSL) followed by the $Kras^{G12D}$ point mutation allele ($Kras^{LSL\text{-}G12D/+}$) were kindly provided by the NCI (Bethesda, MD). By mating $Kras^{LSL\text{-}G12D/+}$ mice and heterozygous Alb-Cre transgenic mice that expressed Cre recombinase under the control of the albumin promoter, hepatocyte-specific Kras-mutated mice [$Kras^{LSL\text{-}G12D/+}$Alb-Cre; called LiK ($Kras^{G12D}$ mutation specifically in the liver) mice] were generated as previously reported (16). C57BL/6 background mice carrying two floxed *mdm2* alleles ($mdm2^{fl/fl}$) and *p53* alleles ($p53^{fl/fl}$) have been previously described (9). Hepatocyte-specific mdm2-knockout Kras-mutated mice [$mdm2^{fl/fl}$ $Kras^{LSL\text{-}G12D/+}$Alb-Cre; called LiKM ($Kras^{G12D}$ mutation and Mdm2 loss in the liver) mice] were generated by mating LiK mice and mdm2-floxed mice. The genotyping of wild-type p53, $p53^{\Delta exons2\text{–}10}$, $p53^{fl}$, wild-type Mdm2, $Mdm2^{\Delta exons5\text{–}6}$, and $Mdm2^{fl}$ alleles was carried out as previously described (19, 20). Hepatocyte-specific mdm2 and p53-double knockout Kras-mutated mice [$p53^{fl/fl}$ $mdm2^{fl/fl}$ $Kras^{LSL\text{-}G12D/+}$Alb-Cre; called LiKMP ($Kras^{G12D}$ mutation and Mdm2/p53 double loss in the liver) mice] were generated by mating LiKM mice and p53-floxed mice. ROSA26-LacZ mice with a C57BL/6 background, which carries LSL-LacZ allele in ROSA26 locus, were purchased from The Jackson Laboratory. To analyze the expression of Cre recombinase in the liver, $Kras^{G12D}$ $Mdm2^{-/-}$ ROSA26-LacZ mice (ROSA26-LacZ $mdm2^{fl/fl}$ $Kras^{LSL\text{-}G12D/+}$Alb-Cre) were generated by mating hepatocyte-specific mdm2-knockout $Kras^{G12D}$ mice and ROSA26-LacZ mice. In these mice, Cre recombinase removes the transcriptional stop codon upstream of LacZ gene. Cre-expressing cells thus express LacZ and are positive for β-galactosidase staining. In addition, LiKMP mice were mated with ROSA26-LacZ mice to generate $Kras^{G12D}$ $Mdm2^{-/-}$ $p53^{-/-}$ ROSA26-LacZ mice (ROSA26-LacZ $mdm2^{fl/fl}$ $p53^{fl/fl}$ $Kras^{LSL\text{-}G12D/+}$Alb-Cre). NOD/Shi-scid/IL2Rγ (null; NOG) mice were previously reported (16, 21). Only male mice were used for all experiments, except for the experiment of $Kras^{G12D}$ $Mdm2^{del/del}$ $p53^{del/del}$ ROSA26-LacZ mice. Mice were maintained in a specific pathogen-free environment and were treated humanely under the approval of the Animal Care and Use Committee of Osaka University Medical School.

Organoid culture

The protocol for murine HPC-derived organoid culture has been previously described (22). For organoid isolation, 0.50 g of nontumorous liver specimens without macroscopic tumors were minced immediately after removal from 6- to 10-week-old mice and digested in DMEM/F-12 (Thermo Fisher Scientific) supplemented with liberase (Roche) and DNase I. After centrifugation of the digestion mixture and washing with Earle's Balanced Salt Solution (Thermo Fisher Scientific), the cell pellet was dissolved in Cultrex PathClear Reduced Growth Factor BME (R&D Systems) and seeded onto a suspension culture microplate (IWAKI). Cells were incubated in isolation culture medium for 10 to 15 days to grow organoids. Organoids were thereafter passaged every 3 to 7 days and cultured in expansion medium. Expansion medium consisted of DMEM/F-12 supplemented with L-glutamine (Thermo Fisher Scientific), 1% antibiotics, B-27 supplement (Thermo Fisher Scientific), N-2 supplement (Thermo Fisher Scientific), N-acetylcysteine (WAKO, Tokyo, Japan), Rspo1 conditioned medium, nicotinamide (Sigma-Aldrich), recombinant mouse EGF (Thermo Fisher Scientific), recombinant human FGF-10 (PeproTech), recombinant human HGF (PeproTech), A83-01 (Sigma-Aldrich), and Y-27632 (FUJIFILM Wako Pure Chemical Corporation). Isolation medium was composed of 70% expansion

medium and 30% wnt-3a conditioned medium supplemented with recombinant human noggin (R&D Systems). Organoids were dissociated into single cells by TrypLE Express (Thermo Fisher Scientific) treatment and repeated pipetting for subsequent experiments.

Data availability

Raw data and processed data of RNA sequencing (RNA-seq) presented were deposited in Gene Expression Omnibus database (GSE201151 (nontumorous liver tissues of LiK and LiKM mice), GSE201593 (AFP-positive or AFP-negative liver tissues of LiKM mice), and GSE201067 [nontumorous liver tissues of LiK and LiKM mice fed normal diet or acyclic retinoid (ACR) diet)]. Other data generated in this study are available within the article and its Supplementary Data files.

Results

Deletion of hepatocyte Mdm2 accelerated liver carcinogenesis in LiK mice

To analyze the influence of constitutive activation of p53 in hepatocytes, we genetically ablated Mdm2 in LiK mice ($mdm2^{fl/fl}$ $Kras^{LSL\text{-}G12D/+}$Alb-Cre; **Fig. 1**). At 4 months of age, all $Kras^{G12D}$ $Mdm2^{del/del}$ (LiKM) mice developed multiple liver tumors, whereas most $Kras^{G12D}$ $Mdm2^{+/+}$ (LiK) mice and $Kras^{G12D}$ $Mdm2^{+/del}$ [LiKM (hetero)] mice did not show macroscopic liver tumors (**Fig. 1A** and **B**). The tumor number, maximum diameter of macroscopic liver tumors, and liver/body weight ratio were significantly increased in the LiKM group in comparison with the other two groups (**Fig. 1A** and **B**). The median survival periods of LiK, LiKM (hetero), and LiKM mice were 319 ± 79, 343 ± 181, and 267.5 ± 199 days, respectively, which was the shortest in the LiKM group (**Fig. 1C**). Tumors were histologically well- to moderately differentiated HCC (**Fig. 1D**), as we previously reported in LiK mice (16). In 6 tumors in 3 mice, the DNA sequence of the hotspots of mutations in the Trp53 gene (exons 5, 6, 7, and 8) was identical to that of spleens, indicating no mutation. mRNA expression of Trp53 and its target genes in liver tumors was not different from that in surrounding nontumorous liver tissues in LiKM mice (Supplementary Fig. S1). LiKM mice were crossed with ROSA26-LacZ mice to generate $Kras^{G12D}$ $Mdm2^{del/del}$ ROSA26-LacZ mice. In these mice, cancer cells were negative for β-galactosidase staining, whereas surrounding nontumorous hepatocytes were positive (**Fig. 1E**). In genotyping PCR, nontumorous liver tissues in $Kras^{G12D}$ $Mdm2^{del/del}$ ROSA26-LacZ mice harbored DNA fragments of $Mdm2^{\Delta exons\ 5/6}$ (**Fig. 1F**). This is the recombination product of the Mdm2-floxed allele by Cre recombinase (19). Tumorous tissues in these mice showed little appearance of this band (**Fig. 1F**). This result indicated that liver tumors in LiKM mice retained Mdm2 gene. Liver tumors developed in LiKM mice were originated from a cell type that is negative for Cre expression.

LiKM mice showed p53 activation and liver inflammation accompanied by upregulation of cytokines and chemokines in the liver

To investigate the mechanisms underlying the accelerated hepatocarcinogenesis in LiKM mice, the phenotypes were analyzed at 6 weeks of age before macroscopic tumor formation. Serum alanine aminotransferase (ALT) and caspase-3/7 activity were elevated in the LiKM mice, indicating liver injury (**Fig. 2A** and **B**). RNA-seq identified 952 upregulated genes and 117 downregulated genes in the livers of target (LiKM) mice in comparison with control (LiK) mice (**Fig. 2C**). On the basis of these genes, "inflammation mediated by chemokine and cytokine signaling pathway" was the most enriched pathway in the PANTHER pathway database (**Fig. 2D**). The apoptosis signaling pathway and p53 pathway were also enriched (**Fig. 2D**). WikiPathways revealed the enrichment of several inflammation-associated pathways in the livers of LiKM mice (**Fig. 2D**). Various inflammation-associated molecules were upregulated in the livers of LiKM mice (**Fig. 2E**). In accordance with these findings, qPCR demonstrated that expression of p53 target genes and inflammation-related genes was elevated in the livers of LiKM mice (**Fig. 2F**). Hepatocytes and nonparenchymal cells (NPC) isolated from the livers of LiKM mice showed that p53 target genes were specifically upregulated in the hepatocyte fraction, whereas p53 mRNA expression was not affected (**Fig. 2G**). p16, a marker of senescence, was also upregulated in hepatocytes from LiKM mice, together with inflammation-related cytokines such as HGF, TNF, IL1β, and Ccl2 (**Fig. 2G**; ref. 23). LiKM mice showed the increase of positive hepatocytes in p53 and p21 IHC, TUNEL staining, and senescence-associated β-galactosidase (SA-β-gal) staining (**Fig. 2H**). IHC for F4/80 and CD3 showed the infiltration of macrophages and T cells, respectively (**Fig. 2H**). Hepatocyte-specific Mdm2 deletion in LiK mice thus induced hepatocyte apoptosis and senescence and provoked liver inflammation.

LiKM mice showed the emergence of HPCs

RNA-seq demonstrated that LiKM mice had enrichment of several stem cell–related pathways in the GeneSigDB database, which especially focuses on cancer and stem cell gene signatures (**Fig. 3A**; ref. 24). Regarding stem cell–related molecules in the liver, several biliary and stem cell–related markers, which are characteristic of HPCs, were upregulated in LiKM mice (**Fig. 3B**). qRT-PCR validated the upregulation of these markers in the livers of LiKM mice, together with various humoral factors known to enhance the expansion of HPCs, such as leukemia inhibitory factor (LIF), oncostatin M (OSM), and IFNγ (**Fig. 3C**). Hepatocytes isolated from the livers of LiKM mice revealed that these factors were upregulated mainly in the hepatocyte fraction (**Fig. 3D**). IHC showed the appearance of cells expressing HPC markers such as CK, AFP, and CD133 in the perivascular areas of the livers of LiKM mice at 6 weeks of age, whereas these cells were not apparent in LiK littermates (**Fig. 3E**). At 4 months of age, IHC showed the expansion of these cells and liver tumors in LiKM mice expressed the characteristic markers of HPCs (**Fig. 3E**). AFP-positive and negative cells were extracted from liver tissues of LiKM mice at 4 months of age for RNA-seq. In AFP-positive cells, Kyoto Encyclopedia of Genes and Genomes pathway gene set enrichment analysis revealed downregulation of Retinol metabolism, which is often observed in the early process of carcinogenesis (25), compared with AFP-negative cells (**Fig. 3F**). These findings suggested the possibility that HPCs were the origin of liver tumors in LiKM mice.

Hepatocyte-specific Mdm2 deletion induced hepatocarcinogenesis, even in the absence of Kras mutation

To examine the impact of hepatocyte-specific deletion of Mdm2 alone, we analyzed the phenotypes of $Kras^{wild}$ $Mdm2^{del/del}$ mice (Mdm2 loss specifically in the liver with wild-type Kras; LiM mice) by comparison with $Kras^{wild}$ $Mdm2^{+/+}$ (wild) mice, which were littermates of the $Kras^{G12D}$ groups analyzed in **Figs. 1–3**. Macroscopic liver tumors were not observed at all, either in the wild group or the LiM group at 4 months of age (Supplementary Fig. S2A and S2B),

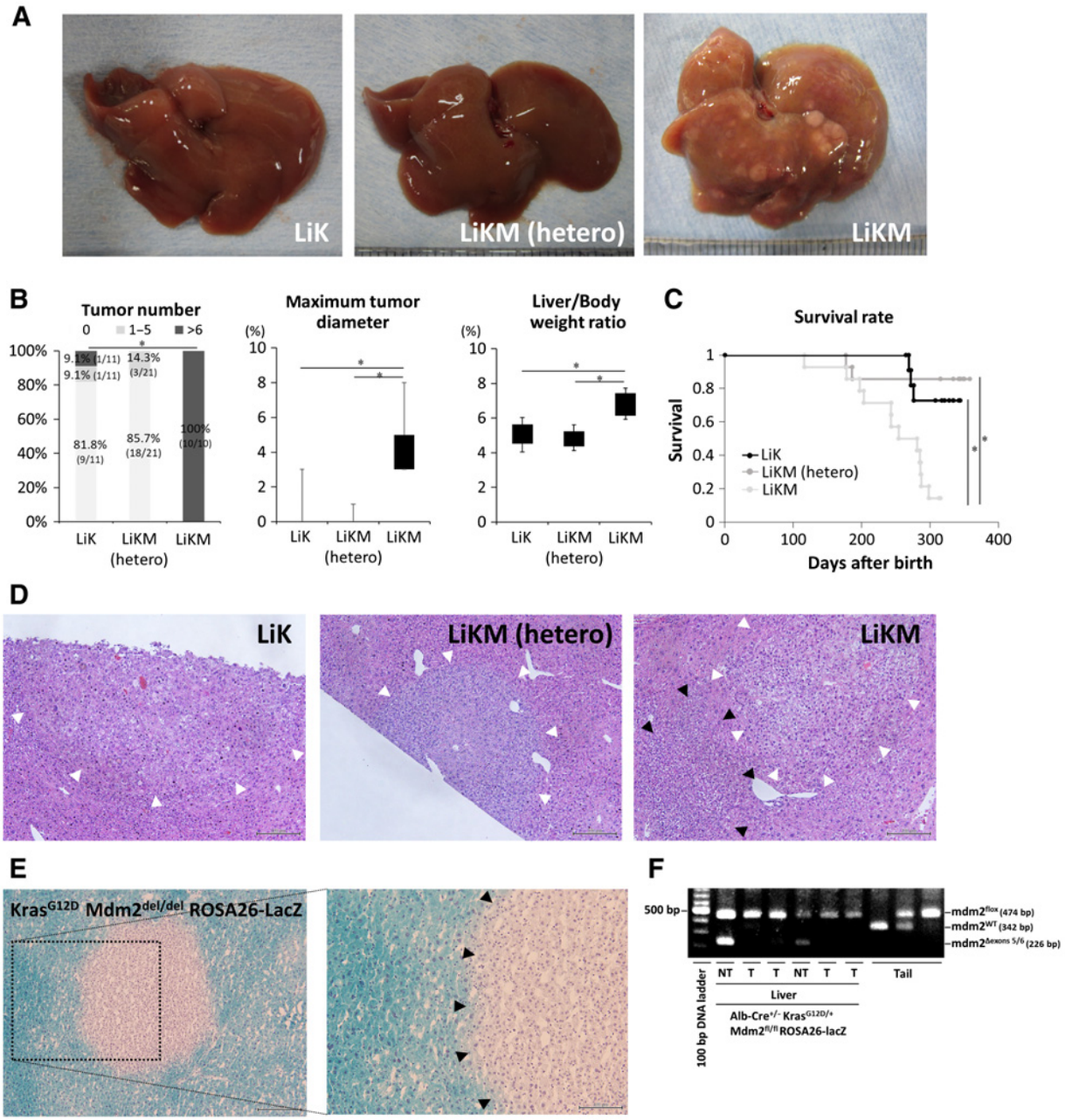

Figure 1.

Hepatocyte-specific Mdm2 deletion in LiK ($Kras^{G12D}$ mutation specifically in the liver) mice promoted the development of liver tumors. Hepatocyte-specific $Kras^{G12D}$-mutant mice [$Kras^{LSL\text{-}G12D/+}$ Alb-Cre; LiK ($Kras^{G12D}$ mutation in the liver) mice] and Mdm2-floxed mice were mated to generate hepatocyte-specific Mdm2-knockout $Kras^{G12D}$ mice. After the mating of $Mdm2^{fl/+}$ $Kras^{+/+}$Alb-Cre mice and $Mdm2^{fl/+}$ $Kras^{LSL\text{-}G12D/+}$ mice, the phenotypes of the following offspring groups were analyzed at 4 months of age (**A**, **B**, and **D**) or subjected to survival analysis (**C**): (i) $Kras^{G12D}$ $Mdm2^{+/+}$ (LiK; $Mdm2^{+/+}$ $Kras^{LSL\text{-}G12D/+}$ Alb-Cre); (ii) $Kras^{G12D}$ $Mdm2^{+/del}$ ($Mdm2^{fl/+}$ $Kras^{LSL\text{-}G12D/+}$ Alb-Cre; LiKM [$Kras^{G12D}$ mutation and Mdm2 loss in the liver)-hetero mice]; and (iii) $Kras^{G12D}$ $Mdm2^{del/del}$ ($Mdm2^{fl/fl}$ $Kras^{LSL\text{-}G12D/+}$ Alb-Cre; LiKM mice) littermates. **A,** Macroscopic appearance of the livers. **B,** Macroscopic tumor number, maximum tumor diameter, and liver to body weight ratio ($N = 10$–21 per group). **C,** Kaplan–Meier survival analysis ($N = 12$–14 per group). **D,** Hematoxylin and eosin staining in the liver (×100). Arrowheads, tumors. **E** and **F,** LiKM mice were mated with ROSA26-LacZ mice, and the $Kras^{G12D}$ $Mdm2^{del/del}$ ROSA26-LacZ offspring mice were sacrificed at 4 months of age. **E,** β-Galactosidase staining of the liver (×100, left; ×200, right). **F,** Genotyping of the Mdm2 gene in tumorous (T) and nontumorous (NT) tissues in $Kras^{G12D}$ $Mdm2^{del/del}$ ROSA26-LacZ mice. Tissue DNA was extracted from both tumorous and nontumorous liver tissues collected via laser microdissection after β-galactosidase staining. The DNA band was separated by electrophoresis after PCR. *, $P < 0.05$.

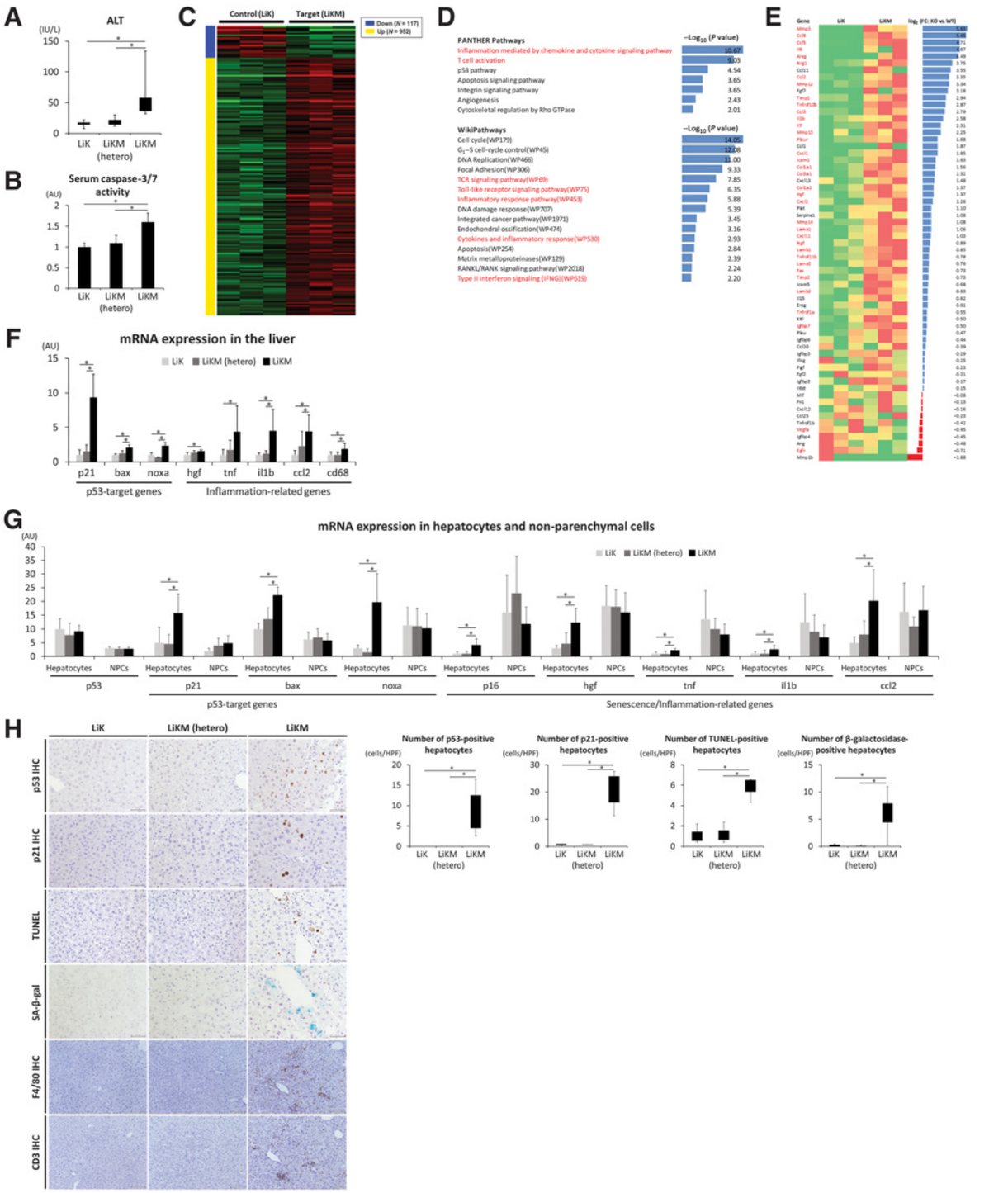

Figure 2.

Mdm2 deletion in hepatocytes induced p53 activation and liver inflammation accompanied by hepatocyte apoptosis, SASP, and inflammatory cytokine production in LiKM mice. Liver samples were obtained from LiK, LiKM-hetero, and LiKM mice at 6 weeks of age. **A,** Serum ALT ($N = 9$ per group). **B,** Serum caspase-3/7 activity ($N = 6$ per group). **C–E,** RNA-seq of the liver tissues in control (LiK) and target (LiKM) mice ($N = 3$ per group). **C,** Heatmap of DEGs. **D,** Enrichment analysis of DEGs in LiKM mice by PANTHER pathways and WikiPathways. Pathways noted in red showed inflammation-associated pathways. **E,** mRNA expression of inflammation-associated molecules. Genes noted in red showed significant expression changes ($P < 0.05$). **F,** qPCR analysis of the mRNA expression in whole liver tissue ($N = 7$–9 per group). **G,** qPCR analysis of the mRNA expression in hepatocytes and NPCs isolated from the liver ($N = 7$–10 per group). **H,** IHC for p53 (×400), p21 (×400), F4/80 (×200), and CD3 (×200), as well as TUNEL staining (×400), and SA-β-gal staining (×400) of the liver and the number of positive hepatocytes ($N = 4$–7). Arrows, positive hepatocytes. *, $P < 0.05$.

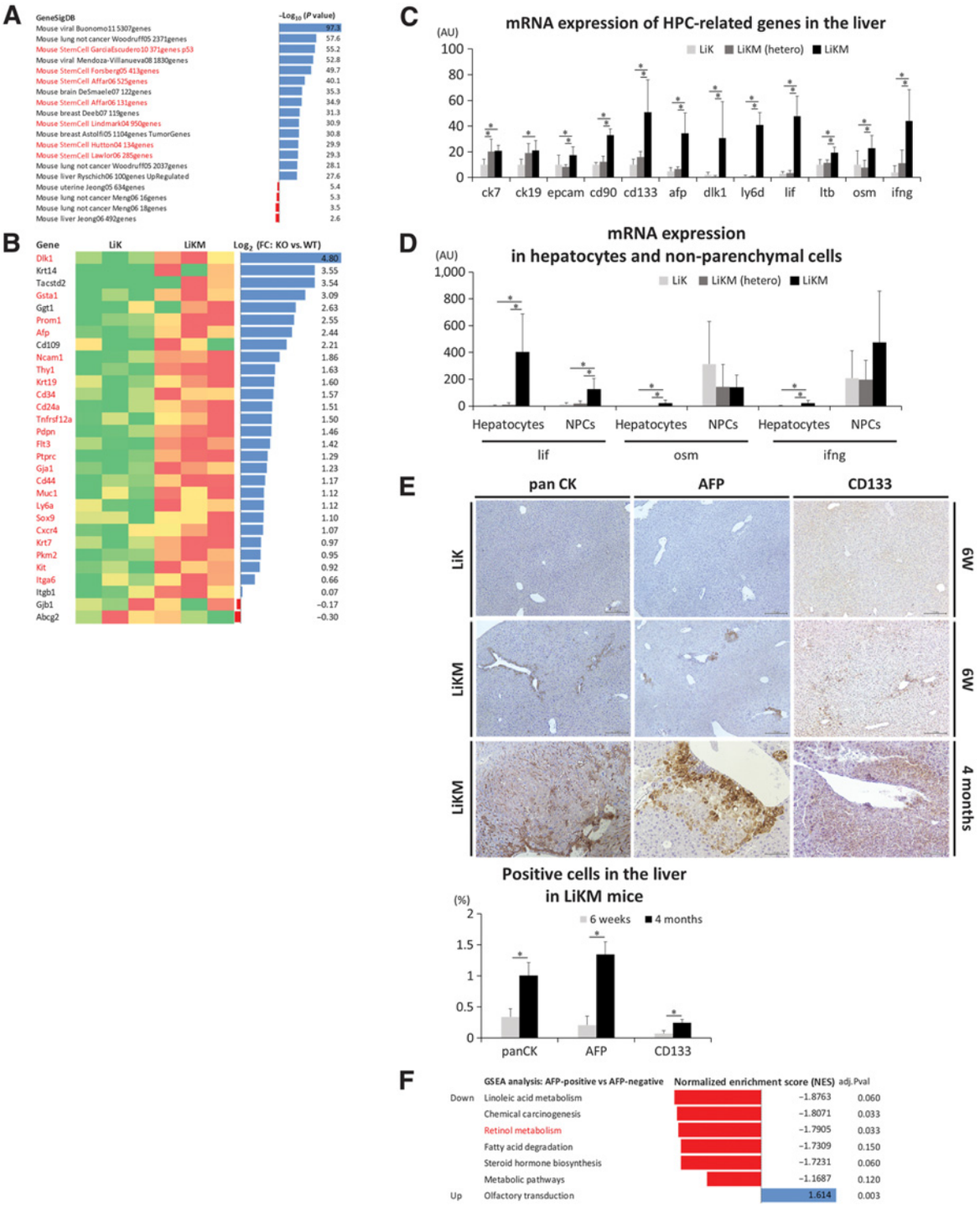

Figure 3.

Mdm2 deletion in hepatocytes induced the emergence of HPCs in LiK mice. Liver samples were obtained from LiK, LiKM-hetero, and LiKM mice at 6 weeks of age (**A**–**E**) or 4 months of age (**E**). **A** and **B,** RNA-seq of liver tissues from LiK and LiKM mice ($N = 3$ per group). Enrichment analysis of DEGs by GenesigDB (**A**). Stem cell–related pathways are shown in red. mRNA expression of HPC markers (**B**). Genes noted in red showed significant expression changes ($P < 0.05$). **C,** qPCR analysis of the mRNA expression of markers of HPC and soluble factors involved in HPC activation in whole liver tissues ($N = 7$–9 per group). **D,** qPCR analysis of the mRNA expression of soluble factors involved in HPC activation in hepatocytes and NPCs isolated from the liver ($N = 6$–10 per group). **E,** IHC for pan CK, AFP, and CD133 in the liver at 6 weeks (×100) and 4 months (×200) of age and frequency of positive cells in the liver in LiKM mice ($N = 3$–4 per group). **F,** Gene set enrichment analysis (GSEA) of AFP-positive cells compared with AFP-negative cells in RNA-seq. AFP-positive and negative cells were extracted from liver tissues of LiKM mice at 4 months of age via laser microdissection. Total RNA was isolated and subjected to RNA-seq ($N = 3$ per group). *, $P < 0.05$.

which was different from the $Kras^{G12D}$ littermates (**Fig. 1A** and **B**). At 6 weeks of age, serum ALT and caspase-3/7 activity were elevated in LiM mice (Supplementary Fig. S2C and S2D). qPCR demonstrated the upregulation of p53 target genes and HPC-related genes in the livers of LiM mice (Supplementary Fig. S2E). Among the inflammation-related genes, namely, hgf, tnf, il-1b, ccl2, and cd68, all of which were upregulated in the livers of LiKM mice (**Fig. 2F**), only ccl2 was upregulated in LiM mice (Supplementary Fig. S2E). Histologic analysis showed an increase in p53-, p21-, TUNEL-, and β-galactosidase–positive hepatocytes; CK-positive HPCs; and CD3-positive T cells in LiM mice, whereas F4/80-positive macrophages were not increased (Supplementary Fig. S2F). We evaluated liver tumorigenesis in wild, $Mdm2^{+/del}$ [LiM (hetero)], and LiM littermates at 2 years of age. Whereas the wild and LiM (hetero) groups showed no tumor development, macroscopic liver tumors were observed in 70% (14/20) of LiM mice (Supplementary Fig. S2G and S2H). Similar to the liver tumors in LiK mice at 4 months of age, liver tumors were histologically well- to moderately differentiated HCC and positive for markers characteristic of HPCs, such as AFP, cytokeratin, and CD133 (Supplementary Fig. S2I). Genotyping PCR showed that liver tumors retained Mdm2 gene, in contrast to nontumorous liver tissues (Supplementary Fig. S2J). Hepatocyte-specific Mdm2 deletion thus promoted liver carcinogenesis even in the absence of the $Kras^{G12D}$ mutation in hepatocytes. $Kras^{G12D}$ mutation in hepatocytes was suggested to augment the inflammatory response and promote liver carcinogenesis induced by Mdm2 deletion.

HPCs in LiKM mice were tumorigenic

We next investigated the tumor-forming ability of HPCs in LiKM mice. Because liver stem/progenitor cells, including HPCs and their precursor of liver "resident" stem cells, can be cultured *ex vivo* as organoids (18, 22), we next generated organoids from nontumorous livers in LiK and LiKM mice. The number of organoids generated from nontumorous liver tissues of LiKM mice was larger than that of LiK littermates (**Fig. 4A**). Compared with isolated hepatocytes, organoids showed extremely high expression of biliary markers and little expression of hepatocyte markers (Supplementary Fig. S3A), which represents the characteristic gene expression pattern of HPCs. Genotyping PCR showed that LiKM organoids retained Mdm2 gene (**Fig. 4B**), indicating the absence of Alb-Cre expression, similar to liver tumors (**Fig. 1E** and **F**). In karyotyping, the percentage of cells with more than 2 lost or gained chromosomes was significantly higher in LiKM organoids in comparison with LiK organoids, suggesting a higher level of chromosomal instability (**Fig. 4C**). Expression of p-Src and Myc oncogenes and pSTAT3 was elevated in organoids from LiKM mice, whereas pErk and pAkt expression, which are downstream of Ras signaling, was not different (**Fig. 4D**). Whereas trp53 expression was lower in LiKM organoids, there was no significant difference in the expression of Trp53-target genes, suggesting no altered p53 activity (Supplementary Fig. S3B). Organoids were subcutaneously allografted to NOG mice, and tumor formation was evaluated 21 days after inoculation. Allografts of LiK organoids were small with a transparent and slightly flesh-colored appearance and were nontumorigenic (**Fig. 4E**). On the other hand, 90.9% (10/11) of LiKM organoids developed large, reddish subcutaneous tumors containing bloody fluid (**Fig. 4E**). Allografts of LiK organoids were mostly composed of gel matrix with little cellular component either by hematoxylin and eosin staining or IHC (**Fig. 4F**). In contrast, allografts of LiKM organoids showed proliferating epithelial-like cells (**Fig. 4F**). Immunohistochemically, these cells were positive for several markers characteristic of HPCs (**Fig. 4F**), which was similar to the liver tumors of LiKM mice (**Fig. 3E**).

ACR induced apoptosis and differentiation of HPCs *in vitro*

ACR is a synthetic oral retinoid with a vitamin A–like structure that binds to retinoid nuclear receptors to activate the transcription of target genes. Because ACR was reported to induce the differentiation and apoptosis of HPCs *in vitro* and to suppress the expansion of HPCs and liver carcinogenesis *in vivo* (26, 27), we analyzed the influence of ACR on tumor development in LiKM mice. *In vitro*, stimulation with ACR upregulated retinoic acid receptors and cell death–related genes and downregulated biliary markers in two cell lines of HPC, WB-F344 and LPC (Supplementary Fig. S4A). The proliferation of these cell lines was suppressed by ACR (Supplementary Fig. S4B), accompanied by the elevation of caspase-3/7 activity in supernatant (Supplementary Fig. S4C). In LiKM organoids, ACR treatment also upregulated retinoid receptor rara and the cell death–related genes p21 and bax (Supplementary Fig. S4D). In addition, ACR downregulated biliary markers and upregulated the hepatocyte marker hnf4a (Supplementary Fig. S4D). *In vitro* proliferation was attenuated by ACR (Supplementary Fig. S4E). ACR administration also suppressed the growth of allograft tumors derived from LiKM organoids (Supplementary Fig. S4F). ACR thus induced apoptosis and differentiation in HPCs and to suppress their proliferation.

ACR suppressed expansion of HPCs and tumor development in LiKM mice

For *in vivo* experiments, LiK or LiKM mice were fed ACR diet or normal diet. In the LiK groups, the ACR diet did not affect liver tumorigenesis (**Fig. 5A** and **B**). In contrast, the ACR diet decreased the tumor number, maximum tumor diameter, and liver/body weight ratio in the LiKM groups (**Fig. 5A** and **B**). Serum ALT levels were not changed by ACR diet (**Fig. 5C**). To analyze the influence of ACR diet, we performed RNA-seq of the nontumorous liver tissues. In normal diet groups, RNA-seq identified 1763 upregulated genes and 167 downregulated genes in the livers of target (LiKM) mice in comparison with control (LiK) mice (**Fig. 5D**). On the basis of these genes, inflammation-related pathways and stem cell–related pathways were enriched in Wikipathways/PANTHER pathways and GenesigDB, respectively, which were similar to the analysis at 6 weeks of age (**Figs. 2D** and **3A**). In LiKM groups, 10 and 70 genes were up- and downregulated in the liver of the ACR group compared with the normal diet group (**Fig. 5E**). In enrichment analysis, a stem cell–related pathway in the GenesigDB database were downregulated in ACR diet group, whereas inflammation-related pathways were not affected (**Fig. 5E**). In qPCR analysis, p53-related genes and senescence/inflammation-related genes in nontumorous liver tissues were not altered by the ACR diet (**Fig. 5F**). Specifically, ACR treatment downregulated several markers that are characteristic of HPCs, including CK7, CK19, EpCAM, CD133, and ly6d, in the LiKM groups, whereas factors known to enhance the expansion of HPCs, such as LIF, OSM, and IFNγ, were not affected (**Fig. 5F**). IHC showed a decrease in HPCs in LiKM mice fed the ACR diet (**Fig. 5G**). ACR thus attenuated HPC expansion and suppressed liver tumorigenesis in LiKM mice.

Constitutive activation of hepatocyte p53 was responsible for the promotion of tumorigenesis in Mdm2-knockout $Kras^{G12D}$ mice

To address whether the acceleration of liver carcinogenesis in LiKM mice was due to p53 activation, we further deleted hepatocyte p53 in LiKM mice (LiKMP mice). Hepatocyte p53 was also knocked out in LiK mice as a reference (LiKP mice). In the LiK groups, hepatic p53 and p21 expression was decreased by p53 knockout in hepatocytes (Supplementary Fig. S5A). The development of liver tumors was promoted

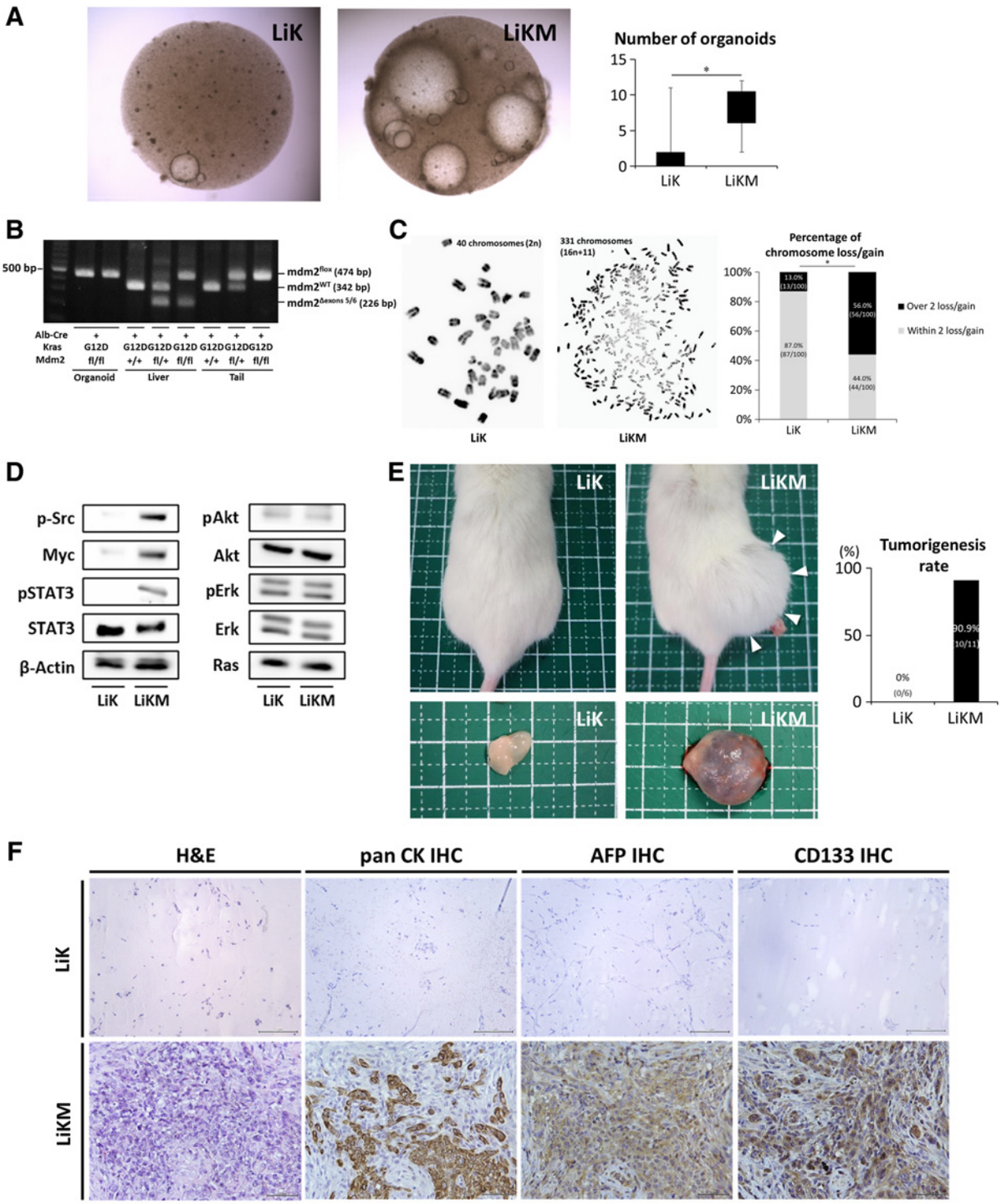

Figure 4.

HPC-derived organoids generated from LiKM mice showed tumor-formation ability in an allograft model. Organoids were generated from 0.50 g liver samples in LiK and LiKM mice. **A,** Representative pictures and numbers of organoids larger than 200 μmol/L 10 days after isolation from the livers ($N = 7$ per group). **B,** PCR of the DNA isolated from the organoids, whole livers, and tails of the indicated genotypes and specimens. **C,** Karyotyping of organoid-consisting cells ($N = 100$ per group). Two lines of organoids were generated in each genotype. Fifty cells were examined for karyotyping in each line. **D,** Protein expression in organoids. **E** and **F,** Organoids were inoculated into NOG mice for allografts. **E,** Macroscopic appearance of mice 21 days after organoid inoculation and the tumorigenesis rate. Arrowheads, allograft. **F,** Hematoxylin and eosin (H&E) staining and IHC for pan CK, AFP, and CD133 in allografts (×400). *, $P < 0.05$.

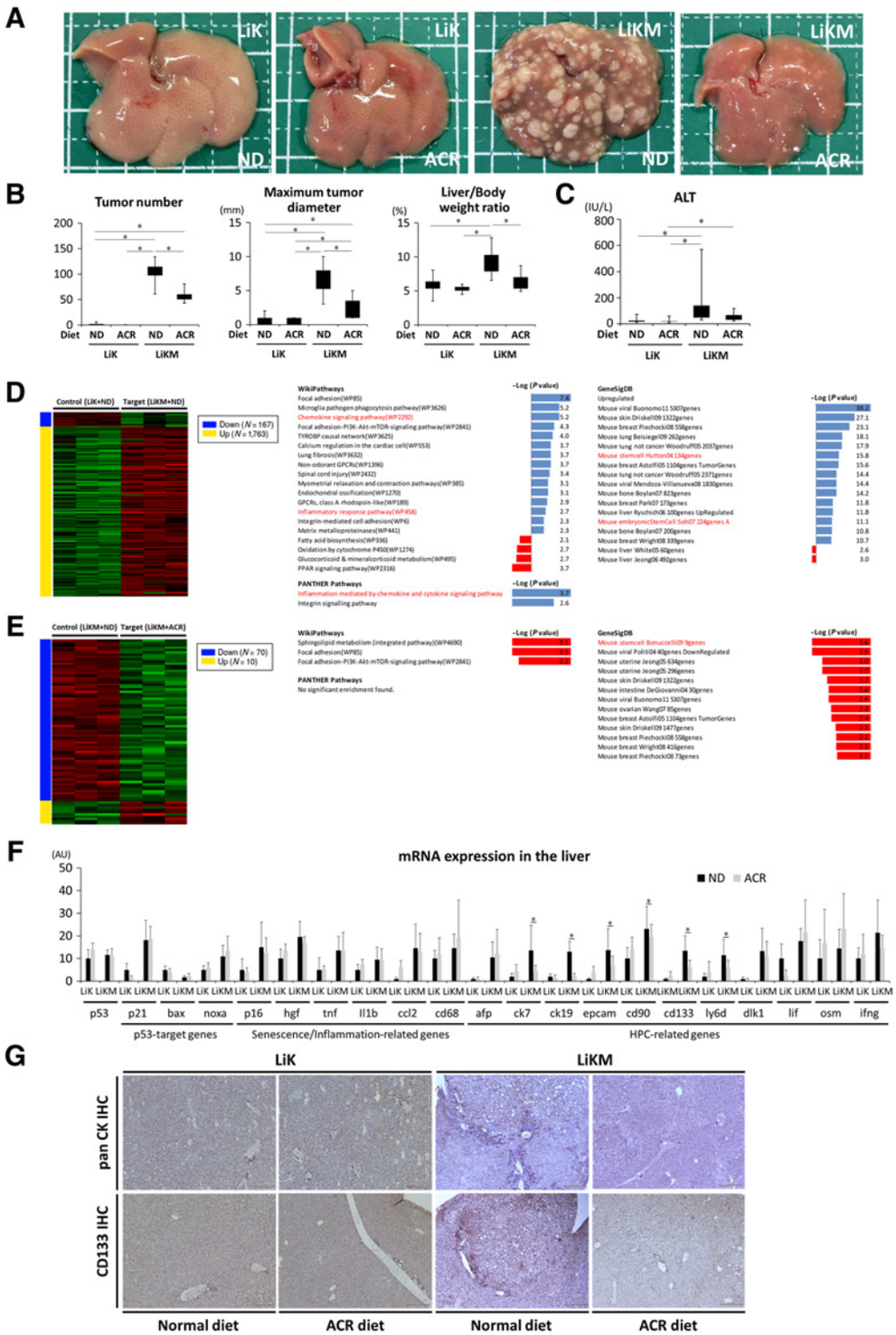

Figure 5.

ACR inhibited HPC expansion and suppressed tumorigenesis in LiKM mice. LiK and LiKM mice were fed a normal diet (ND) or a diet containing 0.06% ACR from 5 weeks of age until sacrifice at 4 months of age. **A,** Representative images of the livers. **B,** Macroscopic tumor number, maximum tumor diameter, and liver to body weight ratio ($N = 14$–17 per group). **C,** Serum ALT ($N = 7$–17 per group). **D** and **E,** RNA-seq of the liver tissues in LiK and LiKM mice ($N = 3$ per group). Total RNA was extracted from nontumorous liver tissues at 4 months of age. Heatmap of DEGs and enrichment analysis between LiK and LiKM mice fed a normal diet (**D**) and LiKM mice fed a normal or ACR diet (**E**). **F,** Pathways noted in red showed inflammation- or stem cell–related pathways. mRNA expression in the liver ($N = 5$–14 per group). **G,** IHC for pan CK and CD133 in the liver (×100). *, $P < 0.05$.

in LiKP mice at 4 months of age (Supplementary Fig. S5B and S5C). Histologically, whereas liver tumors in LiK mice were well- to moderately differentiated HCC, those in LiKP mice were poorly differentiated tumors or cholangiocellular carcinoma composed of tubular and glandular structures (Supplementary Fig. S5D). In the LiKM groups, serum ALT and caspase-3/7 activity were decreased by p53 knockout at 6 weeks of age (**Fig. 6A** and **B**). The expression of p53 and its target genes, senescence/inflammation-related genes, and HPC-related genes was decreased in the livers of LiKMP mice (**Fig. 6C**). IHC showed a decrease in positive TUNEL and SA-β-gal staining and IHC for p53, p21, F4/80, CD3, pan CK, CD133, and AFP (**Fig. 6D**). At 4 months of age, tumor development was suppressed by the knockout of p53 in the LiKM groups (**Fig. 6E** and **F**), which was quite opposite to that of the LiK groups (Supplementary Fig. S5B and S5C). Whereas liver tumors in LiKM mice were well- to moderately differentiated HCC, those in LiKMP mice were poorly differentiated or cholangiocellular carcinoma (**Fig. 6G**), which was the same as those in LiKP mice (Supplementary Fig. S5D). Genotyping PCR showed that liver tumors in LiKMP mice harbored a DNA fragment of $p53^{\Delta exons2-10}$, which was the recombination product of the p53-floxed allele (**Fig. 6H**; ref. 20). A DNA fragment of $Mdm2^{\Delta exons\ 5/6}$ was also observed in liver tumors in LiKMP mice (**Fig. 6H**). LiKMP mice were crossed with ROSA26-LacZ mice, and the liver tissues in offspring $Kras^{G12D}$ $Mdm2^{del/del}$ ROSA26-LacZ $p53^{+/+}$ and $p53^{del/del}$ mice were subjected to β-galactosidase staining. In $Kras^{G12D}$ $Mdm2^{del/del}$ ROSA26-LacZ $p53^{+/+}$ mice, tumor cells of well- to moderately differentiated HCC were negative for β-galactosidase staining, suggesting the absence of Cre expression (**Fig. 6I**). On the other hand, tumor cells both in poorly differentiated tumors and cholangiocellular carcinoma in $Kras^{G12D}$ $Mdm2^{del/del}$ $p53^{del/del}$ ROSA26-LacZ mice were positive for β-galactosidase staining (**Fig. 6I**). This finding suggested that both Mdm2 and p53 were deleted in liver tumors in LiKMP mice. Collectively, all of the phenotypes in LiKM mice, including hepatocyte apoptosis, SASP, liver injury, and increased liver carcinogenesis, were negated by further deletion of hepatocyte p53. Activation of hepatocyte p53 accelerated liver carcinogenesis derived from Cre-negative cell types.

Hepatic p53 activity was correlated with apoptosis, SASP, HPCs and tumor incidence in patients with CLD

We finally analyzed hepatic p53 activity and its significance in CLDs using liver specimens obtained through percutaneous biopsy from patients with CLD and normal liver samples. The flow chart of patient selection is presented in **Fig. 7A**. In accordance with our previous report (9), we adopted p21, one of the most representative p53 target genes, as a marker of p53 activation. The expression of hepatic p21 was elevated in 182 patients with CLD in comparison with 23 patients with normal liver (**Fig. 7B**). Together with p21, a p53 target gene (bax), senescence/inflammation-related genes (p16, hgf, tnf, ccl2, and cd68), and HPC-related genes (cd90, afp, lif, and ifng) were also upregulated in the livers of patients with CLD (**Fig. 7C**). We next performed IHC for HPC markers in the liver samples obtained from surgical hepatectomy for liver metastasis from colorectal cancer (normal liver) or HCC (CLD). Whereas AFP-positive cells were not apparent in normal liver, AFP-positive epithelial cells were present in CLD liver tissues (Supplementary Fig. S6). EpCAM was positive only in cholangiocytes in normal liver (Supplementary Fig. S6). In CLD liver tissues, we observed EpCAM-positive epithelial cells proliferating into liver parenchyma (Supplementary Fig. S6). These findings suggested the presence of HPCs in CLD liver samples. In 182 patients with CLD who underwent percutaneous liver biopsy, p21 mRNA expression was positively correlated with the expression of several p53 target genes (bax and noxa), senescence/inflammation-related genes (p16, hgf, tnf, il-1b, ccl2, and cd68) and HPC-related genes (ck7, ck19 epcam, cd90, cd133, afp, dlk1, lif, osm, and ifng; **Fig. 7D**). Among 182 patients with CLD, we further focused on 144 patients with HCV-related CLDs to analyze the relationship between hepatic p21 expression and tumor incidence after biopsy. These patients were divided into a p21 mRNA-high expression group ($N = 72$) and a p21 mRNA-low expression group ($N = 72$) according to the median p21 mRNA expression value. The cumulative HCC incidence rate after biopsy in the p21-high expression group was significantly higher than that in the p21-low expression group (**Fig. 7E**). Collectively, hepatic p53 activity was increased in patients with CLD and was associated with apoptosis, SASP, HPCs, and liver carcinogenesis.

Discussion

In the current study, we revealed that constitutive activation of hepatocyte p53 accelerated liver carcinogenesis, which is completely opposite to its well-known tumor-suppressive property. Moreover, it should be noted that it was a non–cell autonomous liver carcinogenesis. It was not p53-activated cells that transformed into cancer cells because the cancer cells lacked Cre recombinase expression or Mdm2 deletion (**Fig. 1E** and **F**). Activated p53 executed its intrinsic action as a cell-cycle regulator in hepatocytes, leading to the induction of apoptosis and senescence. By provoking inflammation, activated p53 produces tumorigenic conditions in the liver, where cell types other than p53-activated hepatocytes are likely to malignantly transform. Whereas hepatocytes are the primary epithelial cell population that constitutes almost 80% of the total liver volume, the liver also consists of NPCs such as hepatic stellate cells, macrophages, and endothelial cells. Among the various cell types composing the liver, two cell types have been considered to be tumor-initiating cells of HCC: hepatocytes and HPCs (28, 29).

We demonstrated that p53 activation in hepatocytes provoked the emergence of HPCs (**Figs. 3** and **6**). Although the origin of HPCs is not clearly understood, they are believed to be mainly derived from "resident" stem cells in the liver (17, 18). Whereas HPCs are difficult to observe in the healthy liver, resident stem cells become highly proliferative and expand when regenerative proliferation of mature hepatocytes is impaired under prolonged or extensive liver injury (17, 18). HPCs can differentiate into hepatocytes or cholangiocytes and contribute to liver regeneration (17, 18). Furthermore, the detailed cellular and molecular mechanisms of HPC appearance are not well understood to date. In our experiments, p53 activation in hepatocytes caused liver injury, accompanied by hepatocyte apoptosis and senescence (**Figs. 2** and **6**). Both apoptosis and senescence are irreversible blockades of hepatocyte replication, which could lead to the emergence of HPCs in the case of liver injury. These conditions could have provided the chance for HPCs to expand in LiKM mice. Correlations between p53 activation and apoptosis, senescence, and HPC expansion were also observed in human samples (**Fig. 7**). Our study is the first to demonstrate the association between hepatocyte p53 and HPC expansion. Our findings clarified a part of the cellular and molecular mechanisms of HPC expansion in CLDs.

HPCs were considered to be the origin of liver tumors in LiKM mice on the basis of the following findings. Similar to liver tumors in LiKM mice, liver organoids generated from the stem/progenitor cell population were also negative for Cre expression (**Fig. 4B**) and possessed tumor-formation ability (**Fig. 4E** and **F**). In addition, liver tumorigenesis was suppressed by ACR (**Fig. 5**), which induced the differentiation and apoptosis of HPCs (Supplementary Fig. S4).

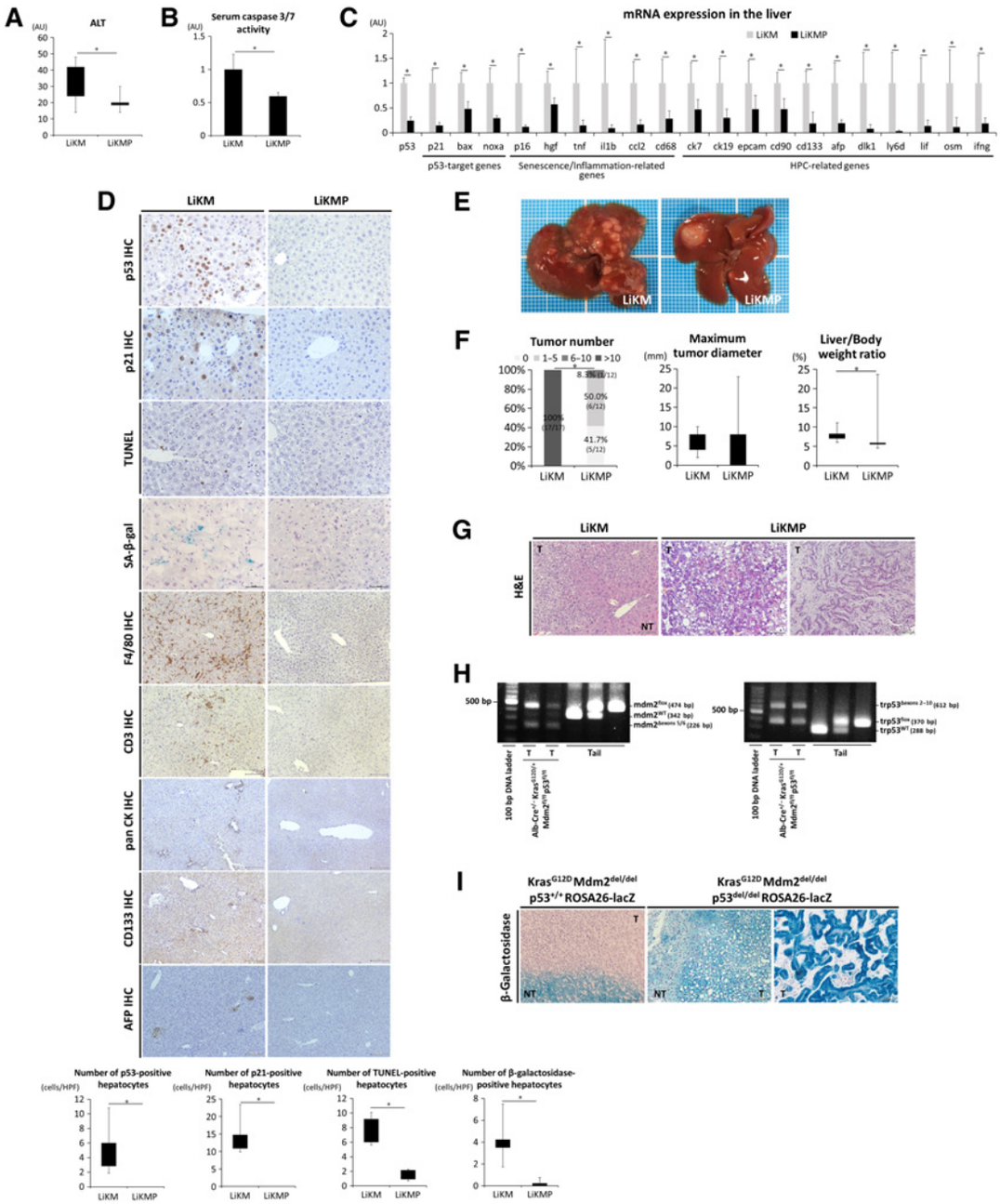

Figure 6.

Concurrent deletion of hepatocyte p53 suppressed hepatocyte apoptosis and SASP, HPC expansion, and development of HCC in LiKM mice. LiKM mice and p53-floxed mice were mated to generate hepatocyte-specific Mdm2 and p53-double knockout $Kras^{G12D}$ mice. After mating $p53^{fl/+}$ $Mdm2^{fl/+}$ $Kras^{+/+}$Alb-Cre mice and $p53^{fl/+}$ $Mdm2^{fl/+}$ $Kras^{LSL\text{-}G12D/+}$ mice, the $Kras^{G12D}$ $Mdm2^{del/del}$ $p53^{+/+}$ ($p53^{+/+}$ $mdm2^{fl/fl}$ $Kras^{LSL\text{-}G12D/+}$ Alb-Cre; LiKM mice) and $Kras^{G12D}$ $Mdm2^{del/del}$ $p53^{del/del}$ [$p53^{fl/fl}$ $mdm2^{fl/fl}$ $Kras^{LSL\text{-}G12D/+}$ Alb-Cre; LiKMP ($Kras^{G12D}$ mutation and Mdm2/p53 double loss in the liver) mice] offspring littermates were sacrificed at 6 weeks (**A–D**) or 4 months (**E–H**) of age. LiKMP mice were mated with ROSA26-LacZ mice to generate $Kras^{G12D}$ $Mdm2^{del/del}$ $p53^{+/+}$ ROSA26-LacZ and $Kras^{G12D}$ $Mdm2^{del/del}$ $p53^{del/del}$ ROSA26-LacZ mice and were sacrificed at 4 months of age (**I**). **A,** Serum ALT ($N = 6$–9 per group). **B,** Serum caspase-3/7 activity ($N = 7$–8 per group). **C,** qPCR analysis of the mRNA expression in whole liver tissue ($N = 6$–9 per group). **D,** IHC for p53 (×400), p21 (×400), F4/80 (×200), CD3 (×200), pan CK (×100), CD133 (×100), and AFP (×100), as well as TUNEL staining (×400) and SA-β-gal staining (×400) of the liver and the number of positive hepatocytes. **E,** Macroscopic images of the livers. **F,** Macroscopic tumor number, maximum tumor diameter, and liver to body weight ratio in the Mdm2-KO groups ($N = 12$–34 per group). **G,** Hematoxylin and eosin (H&E) staining of the liver tissues in LiKM mice and LiKMP mice (left, poorly differentiated tumor; right, cholangiocellular carcinoma; ×200). **H,** Genotyping of the trp53 and mdm2 genes in liver tumors in 4-month-old LiKMP and control mouse tail samples. **I,** β-Galactosidase staining of the livers of $Kras^{G12D}$ $Mdm2^{del/del}$ $p53^{+/+}$ ROSA26-LacZ and $Kras^{G12D}$ $Mdm2^{del/del}$ $p53^{del/del}$ ROSA26-LacZ mice (left, poorly differentiated tumor; right, cholangiocellular carcinoma; ×200). The picture of cholangiocellular carcinoma in $Kras^{G12D}$ $Mdm2^{del/del}$ $p53^{del/del}$ ROSA26-LacZ mice was obtained from a female mouse. *, $P < 0.05$.

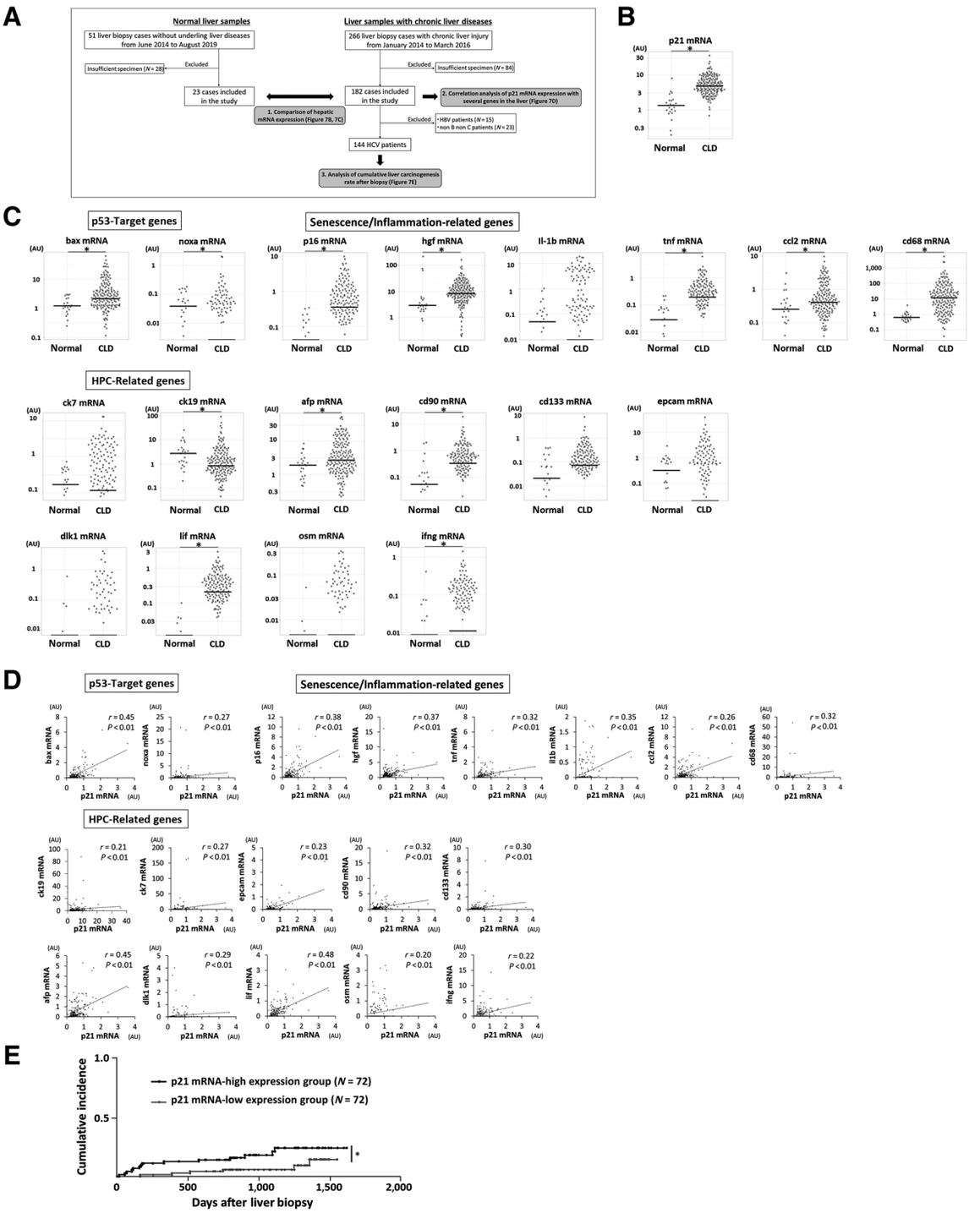

Figure 7.

Hepatic p53 activity was associated with apoptosis, SASP, HPCs, and hepatocarcinogenesis in patients with CLD. Human liver biopsy samples were obtained from 182 patients with CLDs and 23 patients without underlying liver diseases as normal control livers. **A,** Flow chart of patient and sample selection and analysis. **B,** mRNA expression of p21. **C,** mRNA expression of p53 target, senescence/inflammation-related, and HPC-related genes. **D,** Correlation of the mRNA expression in the bulk liver tissues between p53 target, senescence/inflammation-related, and HPC-related genes and p21 in 182 patients with CLD. **E,** Cumulative liver tumor incidence rate of the p21 mRNA-high and p21 mRNA-low expression groups of patients with 144 HCV-related CLDs. Patients were divided into the p21-high expression group ($N = 72$) and the p21-low expression group ($N = 72$) according to the median p21 expression value in the liver. *, $P < 0.05$.

Downregulation of retinol signaling in AFP-positive cells in LiKM mice (**Fig. 3F**) might have suggested the rationale for ACR treatment. Recent accumulating evidence suggests that HPCs can malignantly transform and develop HCC. Several clinical studies revealed that some HCCs were positive for HPC markers and originated from HPCs (30). In several experimental studies, HPCs isolated from both humans and animals were shown to have tumor-formation ability when inoculated into immune-deficient mice (31–33). Regarding genetic abnormalities that underlie their tumor-formation ability, all of these reports demonstrated abnormal karyotypes in tumorigenic HPCs. Our study also showed chromosomal abnormalities in LiKM organoids (**Fig. 4C**), together with tumor-formation ability (**Fig. 4E** and **F**). These findings suggested that HPCs in LiKM mice extracted as organoids harbored characteristics of cancer cells. Chromosomal abnormalities are one of the most common forms of genomic instability in cancers (34). This instability could substantially affect cell physiology and phenotypes, including cell-cycle regulation, metabolism, and protein homeostasis, which might drive carcinogenesis (34). Whereas chromosomal abnormalities might contribute to the tumorigenicity of LiKM organoids, little is known to date about the genetic drivers of HPC-derived HCC (29). HPCs are likely to acquire genetic abnormalities because they are long-lived and highly proliferating cells (17, 18). Similar to previous studies that demonstrated liver carcinogenesis derived from HPCs (31, 35), our LiKM organoids showed increased phosphorylation of STAT3 and Src (**Fig. 4D**), which might provide tumor-formation ability. Nevertheless, further study is needed to identify the critical drivers that induce malignant transformation of HPCs.

Genetic abnormalities can be induced by various environmental stresses. One of the most important factors is chronic inflammation, which is usually accompanied by abundant soluble mediators. In our study, cytokine and chemokine production was revealed to be enriched in p53-activated livers in LiKM mice and patients with CLD (**Figs. 2** and **7**). Among several inflammatory cytokines, TNF is the most studied molecule and has been shown to facilitate tumorigenesis of HPCs (31, 35). In addition to TNFα, multiple humoral factors, such as LT-β, IFNγ, LIF, OSM, HGF, and Ccl2, all of which were upregulated in the livers of LiKM mice (**Figs. 2** and **3**), could accelerate HPC proliferation (36–38). Abundant cytokine production in the liver might contribute to HPC-derived liver carcinogenesis caused by Mdm2 deletion in Kras-mutant mice. Kras mutation activates downstream signaling, such as the Mek/Erk or PI3K/Akt pathways, to enhance cell proliferation and survival, leading to cancer development. Whereas Kras mutation is observed only in 5% to 7% of human HCC (39), the downstream Mek/Erk and Akt/PI3K signaling pathways is activated in more than half of the cases (40, 41). Our hepatocyte-specific $Kras^{G12D}$ mice is a model to activate these pathways and develop liver cancer. Recent studies featured another consequence of Kras activation (42). Kras activation can upregulate various proinflammatory cytokines via activation of the STAT3/NF-kB pathway or enhancement of the SASP, leading to the facilitation of a protumorigenic microenvironment (42). In our model, interestingly, the $Kras^{LSL\text{-}G12D}$ transgene was not considered to be a carcinogenic driver in LiKM mice, because liver tumors did not express Cre recombinase (**Fig. 1E** and **F**). However, the onset of tumor development was accelerated in the presence of $Kras^{G12D}$ mutation in hepatocytes on the basis of the phenotypes of LiM mice at 4 months and 2 years of age (**Fig. 1**; Supplementary Fig. S2). The mechanisms might be partly explained by the enhancement of cytokine production from hepatocytes. Whereas hepatocyte apoptosis and senescence and HPC expansion were observed in LiM mice, some soluble mediators, such as hgf, tnf, il-1b, and ifng, were not upregulated in the livers of LiM mice (Supplementary Fig. S2E), in contrast to LiKM mice. Upregulation of these molecules, especially TNF, might have promoted the tumorigenicity of HPCs to accelerate liver carcinogenesis in LiKM mice. From these findings, constitutive activation of hepatocyte p53, especially in combination with $Kras^{G12D}$ mutation, upregulated various inflammation-associated molecules and created a favorable environment for HPCs to expand and malignantly transform.

In conclusion, whereas loss of the tumor suppressor p53 in hepatocytes increased hepatocarcinogenesis, constitutive activation of p53 also accelerated non–cell autonomous liver tumorigenesis via increased hepatocyte apoptosis, SASP, and progenitor cell activation. It is important to optimize p53 activity in hepatocytes to prevent hepatocarcinogenesis in patients with CLDs.

Authors' Disclosures

H. Hikita reports grants from the Japan Agency for Medical Research and Development, EA Pharma Co., Ltd., Eisai Co., Ltd. and grants from the Japan Agency for Medical Research and Development during the conduct of the study; grants and personal fees from Gilead Sciences, Inc., AbbVie Inc., Otsuka Pharmaceutical Co., Ltd., Chugai Pharmaceutical Co., Ltd., Takeda Pharmaceutical Company Ltd.; personal fees and nonfinancial support from Kowa Company, Ltd.; and grants from ASKA Pharmaceutical Co., Ltd. outside the submitted work. T. Kodama reports personal fees from Eisai Co., Eli Lilly Co., Bayer, Chugai Pharmaceutical Co., MSD, AstraZeneca, Takeda Pharmaceutical, Gilead Sciences Inc, AbbVie and grants from Shionogi Pharma Co., Ltd. outside the submitted work. R. Sakamori reports personal fees from Gilead Sciences, Inc., Merck & Co., ASKA Pharmaceutical Co., Ltd., Sumitomo Pharma Co., Ltd., Otsuka Pharmaceutical Co., Ltd., Chugai Pharmaceutical Co., Ltd., Eisai Co., Ltd., Eli Lilly Japan K.K., Janssen Pharmaceutical K.K., Nihon Pharmaceutical Co., Ltd.; and personal fees from AbbVie Inc. outside the submitted work. J. Kondo reports grants from Japan Society for the Promotion of Science and other support from KBBM, Inc. outside the submitted work. T. Takehara reports grants from the Japan Agency for Medical Research and Development and the Japan Society for the Promotion of Science and nonfinancial support from Kowa Company, Ltd. during the conduct of the study; grants and personal fees from Gilead Sciences, Inc., AbbVie Inc., Otsuka Pharmaceutical Co., Ltd., Chugai Pharmaceutical Co., Ltd., MSD K.K.; personal fees from Kowa Company, Ltd.; grants from EA Pharma Co., Ltd., Eisai Co., Ltd., Takeda Pharmaceutical Company Limited., ASKA Pharmaceutical Co., Ltd., Novo Nordisk Pharma Ltd., Janssen Pharmaceutical K.K.; and grants from Sumitomo Pharma Co., Ltd. outside the submitted work. No disclosures were reported by the other authors.

Authors' Contributions

Y. Makino: Data curation, software, funding acquisition, investigation, visualization, methodology, writing–original draft, project administration. **H. Hikita:** Conceptualization, formal analysis, validation, methodology, writing–review and editing. **K. Fukumoto:** Data curation, software, validation, investigation, visualization, project administration. **J.H. Sung:** Investigation. **Y. Sakano:** Resources. **K. Murai:** Investigation. **S. Sakane:** Investigation. **T. Kodama:** Validation, methodology. **R. Sakamori:** Validation, methodology. **J. Kondo:** Methodology. **S. Kobayashi:** Resources. **T. Tatsumi:** Conceptualization, validation. **T. Takehara:** Conceptualization, supervision, funding acquisition, writing–review and editing.

Acknowledgments

The authors would like to acknowledge Dr. Hiroshi Suemizu (Department of Laboratory Animal Research, Central Institute for Experimental Animals, Kanagawa, Japan) for offering NOG mice. The authors also thank Kowa for kindly providing ACR. They are grateful to Prof. Hidetoshi Eguchi (Department of Gastroenterological Surgery, Osaka University Graduate School of Medicine, Osaka, Japan) for providing surgically resected human liver samples. The authors also thank Miyuki Imai (Department of Gastroenterology and Hepatology, Osaka University Graduate School of Medicine, Osaka, Japan) for technical support. They acknowledge the NGS core facility of the Genome Information Research Center at the Research Institute for Microbial Diseases of Osaka University for the support with RNA-seq and data analysis.

This work was partially supported by a Grant-in-Aid for Early-Career Scientists (to Y. Makino, 19K17432), a Grant-in-Aid for Scientific Research (C) (to Y. Makino, 21K08005), a research grant from the Osaka Cancer Society (to Y. Makino), Grants-in-Aid for Scientific Research (B) (to T. Takehara, JP21H02903) from the Ministry of

Education, Culture, Sports, Science, and Technology, Japan, and a Grant-in-Aid for Research Program on Hepatitis from the Japan Agency for Medical Research and Development (22fk0310512 and JP21fk0210064 to T. Takehara).

The costs of publication of this article were defrayed in part by the payment of page charges. This article must therefore be hereby marked *advertisement* in accordance with 18 U.S.C. Section 1734 solely to indicate this fact.

Note

Supplementary data for this article are available at Cancer Research Online (http://cancerres.aacrjournals.org/).

Received December 23, 2021; revised April 27, 2022; accepted June 8, 2022; published first June 13, 2022.

References

1. Lane DP. Cancer. p53, guardian of the genome. Nature 1992;358:15–16.
2. Bode AM, Dong Z. Posttranslational modification of p53 in tumorigenesis. Nat Rev Cancer 2004;4:793–805.
3. Wade M1, Li YC, Wahl GM. MDM2, MDMX, and p53 in oncogenesis and cancer therapy. Nat Rev Cancer 2013;13:83–96.
4. Totoki Y, Tatsuno K, Covington KR, Ueda H, Creighton CJ, Kato M, et al. Trans-ancestry mutational landscape of hepatocellular carcinoma genomes. Nat Genet 2014;46:1267–73.
5. Meng X, Franklin DA, Dong J, Zhang Y. MDM2-p53 pathway in hepatocellular carcinoma. Cancer Res 2014;74:7161–7.
6. Akyol G, Dursun A, Poyraz A, Uluoglu O, Ataoglu O, Edalý N, et al. P53 and proliferating cell nuclear antigen (PCNA) expression in nontumoral liver diseases. Pathol Int 1999;49:214–21.
7. Loguercio C, Cuomo A, Tuccillo C, Gazzerro P, Cioffi M, Molinari AM, et al. Liver p53 expression in patients with HCV-related chronic hepatitis. J Viral Hepat 2003;10:266–70.
8. Charni M, Rivlin N, Molchadsky A, Aloni-Grinstein R, Rotter V. p53 in liver pathologies-taking the good with the bad. J Mol Med 2014;92:1229–34.
9. Kodama T, Takehara T, Hikita H, Shimizu S, Shigekawa M, Tsunematsu H, et al. Increases in p53 expression induce CTGF synthesis by mouse and human hepatocytes and result in liver fibrosis in mice. J Clin Invest 2011;121:3343–56.
10. Shahnazari P, Sayehmiri K, Minuchehr Z, Parhizkar A, Poustchi H, Montazeri G, et al. The increased level of serum p53 in hepatitis B-associated liver cirrhosis. Iran J Med Sci 2014;39:446–51.
11. Lu W, Lo SY, Chen M, W Kj, Fung YK, Ou JH. Activation of p53 tumor suppressor by hepatitis C virus core protein. Virology 1999;264:134–41.
12. Kao CF, Chen SY, Chen JY, Wu Lee YH. Modulation of p53 transcription regulatory activity and posttranslational modification by hepatitis C virus core protein. Oncogene 2004;23:2472–83.
13. Derdak Z, Lang CH, Villegas KA, Tong M, Mark NM, de la Monte SM. Activation of p53 enhances apoptosis and insulin resistance in a rat model of alcoholic liver disease. J Hepatol 2011;54:164–72.
14. Yuan H, Zhang X, Huang X, Lu Y, Tang W, Man Y, et al. NADPH oxidase 2-derived reactive oxygen species mediate FFAs-induced dysfunction and apoptosis of β-cells via JNK, p38 MAPK and p53 pathways. PLoS One 2010; 5:e15726.
15. Yahagi N, Shimano H, Matsuzaka T, Sekiya M, Najima Y, Okazaki S, et al. p53 involvement in the pathogenesis of fatty liver disease. J Biol Chem 2004;279: 20571–5.
16. Makino Y, Hikita H, Kodama T, Shigekawa M, Yamada R, Sakamori R, et al. CTGF mediates tumor–stroma interactions between hepatoma cells and hepatic stellate cells to accelerate HCC progression. Cancer Res 2018;78:4902–14.
17. Dollé L, Best J, Mei J, Al Battah F, Reynaert H, van Grunsven LA, et al. The quest for liver progenitor cells: a practical point of view. J Hepatol 2010;52:117–29.
18. Köhn-Gaone J, Gogoi-Tiwari J, Ramm GA, Olynyk JK, Tirnitz-Parker JE. The role of liver progenitor cells during liver regeneration, fibrogenesis, and carcinogenesis. Am J Physiol Gastrointest Liver Physiol 2016;310:G143–154.
19. Grier JD, Xiong S, Elizondo-Fraire AC, Parant JM, Lozano G. Tissue-specific differences of p53 inhibition by Mdm2 and Mdm4. Mol Cell Biol 2006;26:192–8.
20. Jonkers J, Meuwissen R, van der Gulden H, Peterse H, van der Valk M, Berns A. Synergistic tumor suppressor activity of BRCA2 and p53 in a conditional mouse model for breast cancer. Nat Genet 2001;29:418–25.
21. Ito M, Hiramatsu H, Kobayashi K, Suzue K, Kawahata M, Hioki K, et al. NOD/SCID/gamma(c)(null) mouse: an excellent recipient mouse model for engraftment of human cells. Blood 2002;100:3175–82.
22. Broutier L, Andersson-Rolf A, Hindley CJ, Boj SF, Clevers H, Koo BK, et al. Culture and establishment of self-renewing human and mouse adult liver and pancreas 3D organoids and their genetic manipulation. Nat Protoc 2016;11: 1724–43.
23. Coppé JP, Desprez PY, Krtolica A, Campisi J. The senescence-associated secretory phenotype: the dark side of tumor suppression. Annu Rev Pathol 2010;5:99–118.
24. Culhane AC, Schwarzl T, Sultana R, Picard KC, Picard SC, Lu TH, et al. GeneSigDB–a curated database of gene expression signatures. Nucleic Acids Res 2010;38:D716–725.
25. Tang XH, Gudas LJ. Retinoids, retinoic acid receptors, and cancer. Annu Rev Pathol 2011;6:345–64.
26. Zheng YW, Tsuchida T, Shimao T, Li B, Takebe T, Zhang RR, et al. The CD133+CD44+ precancerous subpopulation of oval cells is a therapeutic target for hepatocellular carcinoma. Stem Cells Dev 2014;23:2237–49.
27. Guan HB, Nie YZ, Zheng YW, Takiguchi K, Yu HW, Zhang RR, et al. Acyclic retinoid induces differentiation and apoptosis of murine hepatic stem cells. Stem Cell Res Ther 2015;6:51.
28. Marquardt JU, Andersen JB, Thorgeirsson SS. Functional and genetic deconstruction of the cellular origin in liver cancer. Nat Rev Cancer 2015;15:653–67.
29. Sia D, Villanueva A, Friedman SL, Llovet JM. Liver cancer cell of origin, molecular class, and effects on patient prognosis. Gastroenterology 2017;152: 745–61.
30. Ziol M, Nault JC, Aout M, Barget N, Tepper M, Martin A, et al. Intermediate hepatobiliary cells predict an increased risk of hepatocarcinogenesis in patients with hepatitis C virus—related cirrhosis. Gastroenterology 2010; 139:335–43.
31. Li XF, Chen C, Xiang DM, Qu L, Sun W, Lu XY et al. Chronic inflammation-elicited liver progenitor cell conversion to liver cancer stem cell with clinical significance. Hepatology 2017;66:1934–51.
32. Yoshimura H, Harris R, Yokoyama S, Takahashi S, Sells MA, Pan SF, et al. Anaplastic carcinomas in nude mice and in original donor strain rats inoculated with cultured oval cells. Am J Pathol 1983;110:322–32.
33. Zhang A, London R, Schulz FM, Giguère-Simmonds PW, Delriviere L, Chandraratana H, et al. Human liver progenitor cell lines are readily established from nontumorous tissue adjacent to hepatocellular carcinoma. Stem Cells Dev 2010;19:1277–84.
34. Baudoin NC, Bloomfield M. Karyotype aberrations in action: the evolution of cancer genomes and the tumor microenvironment. Genes 2021; 12:558.
35. Jing Y, Sun K, Liu W, Sheng D, Zhao S, Gao L, et al. Tumor necrosis factor-α promotes hepatocellular carcinogenesis through the activation of hepatic progenitor cells. Cancer Lett 2018;434:22–32.
36. Erker L, Grompe M. Signaling networks in hepatic oval cell activation. Stem Cell Res 2007;1:90–102.
37. Viebahn CS, Benseler V, Holz LE, Elsegood CL, Vo M, Bertolino P, et al. Invading macrophages play a major role in the liver progenitor cell response to chronic liver injury. J Hepatol 2010;53:500–7.
38. Viebahn CS, Tirnitz-Parker JE, Olynyk JK, Yeoh GC. Evaluation of the "Cellscreen" system for proliferation studies on liver progenitor cells. Eur J Cell Biol 2006;85:1265–74.
39. Pylayeva-Gupta Y, Grabocka E, Bar-Sagi D. RAS oncogenes: weaving a tumorigenic web. Nat Rev Cancer 2011;11:761–74.
40. Ito Y, Sasaki Y, Horimoto M, Wada S, Tanaka Y, Kasahara A, et al. Activation of mitogen-activated protein kinases/extracellular signal-regulated kinases in human hepatocellular carcinoma. Hepatology 1998; 27:951–8.
41. Calvisi DF, Ladu S, Gorden A, Farina M, Conner EA, Lee JS, et al. Ubiquitous activation of Ras and Jak/Stat pathways in human HCC. Gastroenterology 2006; 130:1117–28.
42. Hamarsheh S, Groß O, Brummer T, Zeiser R. Immune modulatory effects of oncogenic KRAS in cancer. Nat Commun 2020;11:5439.